# Structural Signatures of Type IV Isotherm Steps: Sorption of Trichloroethene, Tetrachloroethene, and Benzene in Silicalite-I

**N. Floquet,*,† J. P. Coulomb,† G. Weber,‡ O. Bertrand,‡ and J. P. Bellat‡**

*C.R.M.C2, CNRS, Campus de Luminy, Case 901, 13288 Marseille Cedex 9, France, and L. R. R. S., CNRS, Université de Bourgogne, B. P. 400, 21011 Dijon Cedex, France*

*Received: February 28, 2002; In Final Form: July 10, 2002*

We have investigated by in situ neutron diffraction the structural properties of $C_2HCl_3$, $C_2Cl_4$, and $C_6D_6$ sorbed phases in silicalite-1. Our motivation is to correlate the structure of these three confined species to the fact that their adsorption isotherms are characterized by no step, one step, and two steps, respectively. From our detailed neutron diffraction investigation, we deduce that the adsorption isotherm steps are not signatures of phase transitions but are correlated to the different adsorption stages observed during the silicalite-1 loading. For $C_6D_6$, such a loading is a three stage process (the $C_6D_6$ molecules fill successively, the intersections, then the straight channels and the sinusoidal channels by forming dimers and then interconnecting monomer chains). Concerning $C_2Cl_4$, it is a two stage process (the $C_2Cl_4$ molecules fill the intersections and after indifferently the straight channels and the sinusoidal channels). Usual sorption is observed for $C_2HCl_3$, which fills all parts of the silicalite-1 porosity indifferently. In addition, this comparative study highlights that a step-filling process takes place in the silicalite-1 as far as the symmetry of the sorbed molecule is concerned.

## 1. Introduction

Usually, the sorption isotherms in zeolite belong to type-I. Nevertheless, almost two decades ago, a step (which is characteristic of type IV isotherms) was observed in the sorption isotherms of tight-fitting molecules (such as *p*-xylene or $C_6D_6$) in silicalite-1.[1,2] In addition, an exothermic peak associated to that step was observed in the microcalorimetric signal.[3] Steps and substeps have also been observed during the sorption of a large number of smaller molecules (ranging from $H_2$ to Kr).[4−7] The conclusive existence of the sorbed phase transition has been pointed out from the comparison of the structural analysis between $^{40}Ar-^{36}Ar$ sorbed species in silicalite-1.[8] The two sorbed phases, which characterize the phase transition, are a fluid phase and a commensurate solid phase. By analogy, the results obtained upon adsorption of tight-fitting molecules on silicalite have been interpreted as the signature of a sorbed phase transition.[2,9] Today, these systems have been examined by several experimental techniques[10] and have been investigated from different theoretical studies.[11] There are still discrepancies in all of the reported results; nevertheless, the general recent trend is to correlate unusual calorimetric features to an adsorption by steps of the sorbed aromatic molecules associated to the site heterogeneity in silicalite-1.[12−14]

For this study, we chose to investigate the adsorption in silicalite-1 of the three molecules $C_2HCl_3$, $C_2Cl_4$, and $C_6D_6$ because their adsorption isotherms present no step (type I isotherm), one step, and two steps (type IV isotherms), respectively, as shown in Figure 1.[12,15,16]

Calorimetric measurements on $C_2HCl_3$/silicalite-1 and $C_2Cl_4$/silicalite-1 systems were performed by Bouvier et al.[15,17] It appears that in the case of the two chloroalkene molecules of similar size (L × l × h = 6.8 Å × 6.6 Å × 3.6 Å), $C_2HCl_3$ adsorption has the features of smaller molecules such as $CH_4$, Xe, and $C_2H_6$ (4.2 Å < ∅ < 5.4 Å), while $C_2Cl_4$ adsorption has the features of aromatic molecules such as *p*-xylene (∅ > 6.0 Å). Calorimetric data on the $C_6H_6$/silicalite-1 system were reported by several authors.[3,16,18] The interpretation of the two steps observed in the adsorption isotherm is still open. Even the recent experimental studies performed by complementary techniques, X-ray and neutron diffraction[19] and FT-Raman,[10] report again different interpretations of the locations of benzene molecules at loadings higher than four. Obviously, it seems that the discrepancies in the experimental results and/or their interpretations will remain as far as the structural or spectroscopic characterizations will not be recorded simultaneously with the adsorption isotherm that measures the true adsorption capacity of the silicalite-1 sample used.

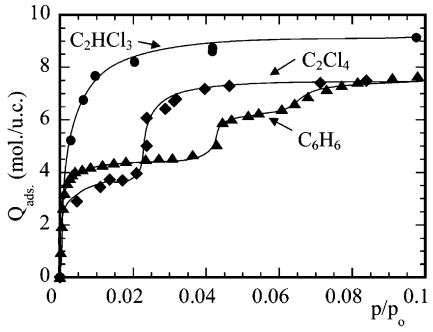


**Figure 1.** Adsorption isotherms of trichloroethene, tetrachloroethene, and benzene sorbed phases in silicate-1 at $T = 298$, 298, and 183 K, respectively.[12,15,16]

In this in situ neutron diffraction study, we have recorded diffraction patterns and adsorption isotherms simultaneously. For each system, we tried first to find out the main diffraction signatures of the adsorption and second to determine the mean location of the sorbed molecules in the silicalite-1 porosity by

* To whom correspondence should be addressed. E-mail: floquet@crmc2.univ-mrs.fr.
† Campus de Luminy.
‡ Université de Bourgogne.

10.1021/jp025701s CCC: $25.00 
Published on Web 12/17/2002

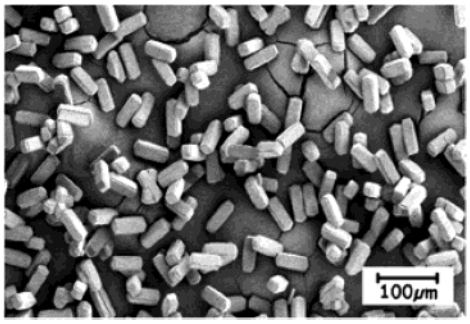


**Figure 2.** Scanning electron micrograph of our silicalite-1 sample.

the Rietvelt method analysis of all the diffraction patterns recorded at increasing loading.

## 2. Experimental Section

The silicalite-1 sample was synthesized at the Laboratoire des Materiaux Mineraux (Mulhouse-France). The scanning electronic micrograph represented in Figure 2 points out that our sample was composed of well-shaped crystals with a narrow size distribution. The neutron diffraction experiments were performed at the Laue Langevin Institute, on the two axis D1-B diffractometer. The diffractograms were recorded between 0.08 $Å^{-1} \leq Q \leq 3.38$ $Å^{-1}$. Two silicalite-1 samples, of the same mass ($m = 2.05$ g), were used. Prior to the neutron diffraction analysis, the samples were outgazed under vacuum ($P < 10^{-6}$ Torr) at $T = 523$ K during around 12 h. Calibration adsorption isotherms were measured at $T = 273$ K during the neutron experiment to determine the sorption loading with high accuracy.

## 3. Results and Discussion

Three main adsorption phenomena could take place during the sorption of molecules in silicalite-1: (i) the transition of the confined phase between a fluid phase and a solid (commensurate or not) phase;[4−8] (ii) the silicalite-1 structure transition between the monoclinic structure (named MONO) and the two orthorhombic structures (named ORTHO and PARA);[9,20−22] (iii) the cooperative change of locations of the sorbed molecules within the silicalite-1 porosity induced by the existence of three kinds of adsorption sites: channel intersections (I), straight channels (S), and zigzag channels (Z).[13,14,23,24]

These three adsorption phenomena give rise, on the diffraction patterns recorded at increasing loading (Figure 3), to specific features that we looked for systematically. For this purpose, all of the powder neutron diffraction patterns were analyzed by the Rietvelt method[25] starting from the neutron diffraction data reported for the empty dehydrated silicalite-1.[20]

The most important intensity modifications of the diffraction peaks are for the two first peaks located at low $Q$ (0.5−0.7 $Å^{-1}$) and the peaks located at medium $Q$ (1.6−1.75 $Å^{-1}$). To show the main modifications of the diffractograms as a function of the increasing loading, the diffractograms presented in Figure 3 are limited between $Q = 0.4$ and 2.6 $Å^{-1}$.

These systems are characterized by a high scattering length of the sorbed molecules ($b_{C_2HCl_3} = 38.3 \times 10^{-13}$ cm, $b_{C_2Cl_4} = 51.6 \times 10^{-13}$ cm, $b_{C_6D_6} = 79.9 \times 10^{-13}$ cm) as compared to a high-diffusing molecule such as argon ($b_{36Ar} = 26.9 \times 10^{-13}$ cm) and to the silicalite framework ($b_{SiO_2} = 15.7 \times 10^{-13}$ cm). Thus, the mean location of the sorbed molecules within the porosity is a parameter much more sensitive toward the modification of the peak intensity of the diffraction pattern as compared to the small change of the atomic positions of the silicalite framework as it has recently been proved.[19]

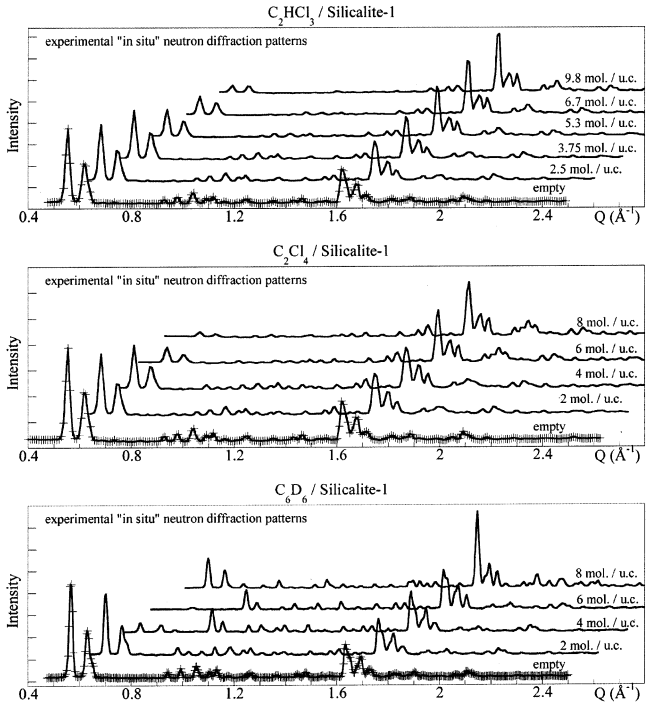


**Figure 3.** Experimental in situ neutron diffraction patterns recorded at increasing loading of $C_2HCl_3$, $C_2Cl_4$, and $C_6D_6$, respectively, in silicalite-1.

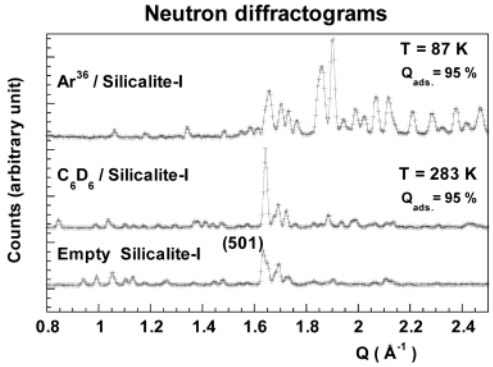


**Figure 4.** Neutron diffractograms of $^{36}Ar$ and $C_6D_6$ confined phases in silicalite-1 at high loading ($Q_{ads} = 95\%$) and at $T = 87$ K and $T = 283$ K, respectively.

**Sorbed Phase Transition.** First analysis consists to determine if new diffraction peaks arise on the patterns as a function of the loading. For the three molecules $C_2HCl_3$, $C_2Cl_4$, and $C_6D_6$, no additional diffraction peak is observed for every loading. Figure 4 shows the pattern of $C_6D_6$ /silicalite-1, which is compared to the empty silicalite-1 pattern and to the $^{36}Ar$ /silicalite-1 pattern where new strong peaks are present in the $Q$ range: 1.85−1.95 $Å^{-1}$. In the case of Ar adsorption in silicalite-1, these new additional peaks are the signature of the Ar-confined phase transition between a fluid phase and a commensurate solid phase.[8] The first finding is that isotherm steps observed for $C_2Cl_4$ and $C_6D_6$ adsorption are not the signatures of confined phase transition.

**Silicalite-1 Structure Transition.** The second analysis consists of measuring the change of position of the diffraction peaks during sorption. Because of the very good resolution, peak shifts and splittings are clearly observed by X-ray diffraction in the $Q$ range: 1.60−1.95 $Å^{-1}$ as previously reported in the case of the adsorption of these three molecules and other aromatic molecules such as *p*-xylene. Figure 5 shows the X-ray patterns recorded at increasing $C_2HCl_3$ loading corresponding

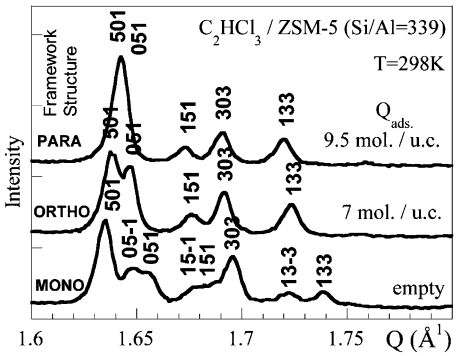


**Figure 5.** In situ X-ray diffractograms of $C_2HCl_3$ sorbed molecules in silicalite-1 at $T = 298$ K and at three loading $Q_{ads} = 0$, 7, and 9.5 mol/uc, respectively.[26]

to the three structural phase of the silicalite-1 (named MONO, ORTHO, and PARA).[26] Such accurate characterization is not allowed from neutron diffraction as underlined by the recent diffraction study of Goyal et al.[19]

However, another way to give evidence of silicalite-1 structure change (and/or its framework flexibility) from neutron diffraction patterns is to determine the silicalite-1 cell parameters as a function of the loading. As shown by the three plots drawn in Figure 6, the unit cell parameter deviations are of the order of 0.5% or less as observed in the case of *p*-xylene adsorption in silicalite.[27] The evolution of the cell parameters presents variations for the three systems: the c parameter is constant for $C_2HCl_3$ near $Q_{ads} = 7$ mol/uc. It is related to the MONO−ORTHO phase transition. Three distinct variations are observed at $Q_{ads} = 2$, 4, and near 7 mol/uc in the case of $C_2Cl_4$ and $C_6D_6$. Those observed at $Q_{ads} = 4$ and near 7 mol/uc correspond, respectively, to the MONO−ORTHO and ORTHO−PARA phase transitions.

The second finding is that silicalite-1 phase transitions (largely reported by many authors) are clearly evidenced in the case of the three sorbed $C_2HCl_3$, $C_2Cl_4$, and $C_6D_6$ molecules.

**Stage-Filling Process of the Sorbed Molecules.** The third analysis consists of measuring the evolution of the intensity of all of the diffracted peaks as a function of the loading. The results for the three sorbed molecules are reported on the plots drawn in Figure 7. The relative intensities $I_{(101)(011)r}$ and $I_{(200)(020)r}$ of the two first highest double peaks [(101)(011)] and [(200)-(020)] are decreasing for the three molecules, up to near 0.1 for $C_2HCl_3$ at $Q_{ads} = 10$ mol/uc, near 0 for $C_2Cl_4$ at $Q_{ads} = 8$ mol/uc. In the case of $C_6D_6$, $I_{(101)(011)r}$ and $I_{(200)(020)r}$ decrease up to 0 at $Q_{ads} = 6$ mol/uc, then increase up to near 0.35 at $Q_{ads} = 8$ mol/uc, with an intensity inversion as pointed out in Figure 8. A similar intensity variation is observed for the two single peaks (102) and (002), but a strong intensity increase is measured for the third highest peak [(501)(051)]. Such intensity variations as a function of the loading are observed for all of the peaks of the diffractograms. Monotonic intensity variations are expected for a homogeneous filling of the whole silicalite porosity whatever is the sorbed molecule as shown in Figure 9.

For a single peak (*hkl*), the relative intensity is $I_{hklr} = (1 + \alpha Q_{ads})^2$ and for a double peak $(hkl)_1$ $(hkl)_2$, the relative intensity $I_{(hkl)1(hkl)2r} = I_{(hkl)1r} + I_{(hkl)2r} = 1 + \beta Q_{ads} + \gamma (Q_{ads})^2$ where $\alpha$, $\beta$, and $\gamma$ are constants characteristic of the adsorbed molecules (their scattering lengths and their positions within the silicalite porosity). The intensity discontinuities observed at $Q_{ads} = 4$ mol/uc for the three sorbed molecules and even at $Q_{ads} = 7$ mol/uc for $C_6D_6$ in the experimental plots clearly indicate a change of the porosity filling mode.

To determine this change of location of the sorbed molecules inside the silicalite porosity, all diffracted patterns were analyzed by the Rietvelt method using the program Fullprof. For the three

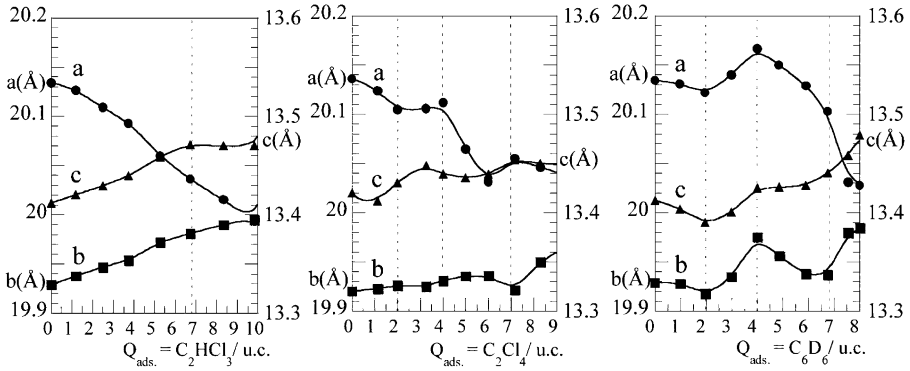


**Figure 6.** Silicalite unit cell parameters (a, b and c) as a function of $C_2HCl_3$, $C_2Cl_4$, and $C_6D_6$ loading, respectively, determined from neutron diffraction patterns.

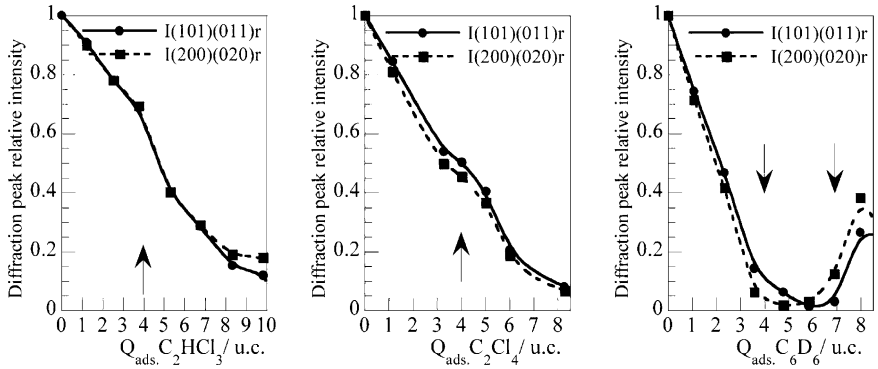


**Figure 7.** Relative intensity of the double diffraction peaks (101)(011) and (200)(020) of silicalite-1 as a function of $C_2HCl_3$, $C_2Cl_4$, and $C_6D_6$ loading, respectively, determined from neutron diffraction patterns.

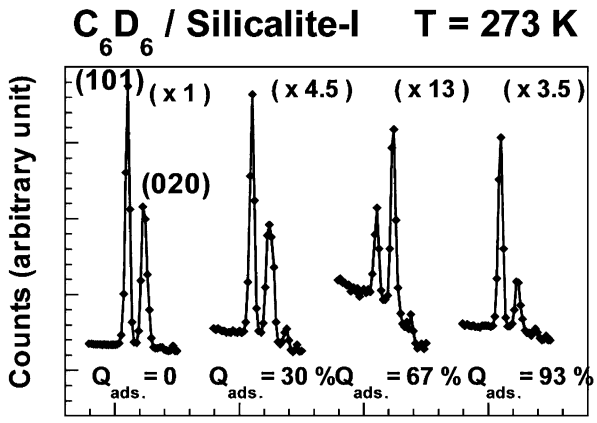


**Figure 8.** Intensities of the double diffraction peaks (101)(011) and (200)(020) as a function of $C_6D_6$ loading in silicalite-1 at $T = 273$ K.

systems, the sorbed phases are not commensurate solid phases (as in the case of argon[8]), but they are mobile phases localized within the three kinds of porosity named I, S, and Z. From a structural viewpoint, each system cannot be seen as a stoichiometric complex as defined by Mentzen et al.,[28] whatever is the loading. Then, the standard conditions used in the Rietvelt method have to be adapted to the specificities of these particular systems.

For each system, the diffraction patterns were refined using a maximum of 10 independent molecule locations to take into account the disorder of their positions in the silicalite porosity. The silicalite atom coordinates obtained by van Koningsvelt[20] and the space group *Pnma* were chosen for the refinement for empty silicalite and for each loading. Any deviations from *Pnma* symmetry appear to be insignificant owing to the limited nature of our neutron diffraction data.[19] For empty silicalite-1, the refinements converged to correlation *R* factors $R_{wp} \approx 10\%$, the coordinates of the framework atoms being restrained. For loaded silicalite-1, idealized models of the sorbed molecules were used and rigid body restraints were applied to them (the molecule was allowed to move and to rotate from its center of mass during the refinement). In some case, refinements could converge to several close sets of positions of the adsorbed molecules, seeing that the flexibility of the silicalite framework and the fact to have in such system a small amount of molecules at random positions were not considered. For each pattern, we chose the set of adsorbed molecule positions with respect to the best fit of the calculated patterns and the suitable geometrical details of the refined models.

**Case of $C_2HCl_3$.** Experimental patterns for $C_2HCl_3$/silicalite system recorded at increasing loading and patterns resulting from Rietvelt refinement corresponding to the best correlation *R* factors ($R_{wp} \approx 10\%$) are given in Figures 3 and 10, respectively.

At low loading, at $Q_{ads} = 1.2$, 2.5, and 3.75 mol/uc, respectively, $C_2HCl_3$ molecules converge to three independent locations as shown in Figure 11. The first one is close to the channel intersections, with its center at $y = 0.19$ and standing nearly vertically to the (010) mirror plane (I). The second one is in the straight channel at $y = 0.10$ and tilted at $\approx 55°$ to the mirror plane (S). The third one is in the zigzag channel at $y = 0.21$ and tilted at $\approx 30°$ to the mirror plane (Z). The occupancies for the three $C_2HCl_3$ positions are roughly equal. At $Q_{ads} = 3.7$ mol/uc, these occupancies are 1.5, 1.1, and 1.1 per unit cell, respectively. It appears that at low loading, $C_2HCl_3$ molecules occupy the three kinds of site of the silicalite-1 porosity.

At a higher loading, at $Q_{ads} = 5.3$, 6.7, 8.3, and 9.8 mol/uc, respectively, $C_2HCl_3$ molecules still occupy three independent locations with the same ratio of occupancy (Figure 11). The first one in the channel intersection moved near zigzag opening at $y = 0.24$ and tilted to be nearly parallel to the (010) mirror plane (IZ). The second one in the straight channel at $y = 0.10$ is more centered and stands nearly vertical to the (010) mirror plane (IS). The third one in the zigzag channel is at $y = 0.25$ and lies parallel to the (010) mirror plane (Z). At $Q_{ads} = 9.8$ mol/uc, the occupancies are 2.7, 4, and 3.1 per unit cell, respectively. It means that at higher loading, $C_2HCl_3$ molecules still occupy the three kinds of site. Moreover, the molecule orientation that is perpendicular or parallel to the (010) mirror plane indicates the high coupling between molecules themselves and silicalite-1 framework.

These findings give an interpretation to the calorimetric results (Figures 1 and 12) obtained by Bouvier et al.[15,17] A more or less homogeneous filling of the silicalite porosity on the three kinds of sites gives rise to type I isotherm with no step (Figure 1), a continuous increase of its adsorption enthalpy, and a continuous decrease of its adsorption entropy (Figure 12). It comes out that the silicalite phase transition MONO−ORTHO arising at $Q_{ads} = 7$ mol/uc has no calorimetric signature. Moreover, it does not correspond to the molecule rearrangement observed at $Q_{ads} = 5.3$ mol/uc as it would be expected.

**Case of $C_2Cl_4$.** Figures 3 and 13 show the experimental patterns for the $C_2Cl_4$/silicalite system recorded at increasing loading and patterns resulting from Rietvelt refinement, respectively.

At low loading, at $Q_{ads} = 1.1$, 2.0, 3.3, and 4.0 mol/uc, respectively, $C_2Cl_4$ molecules converge to only one independent location denoted IS in Figure 14. It is between the channel intersection and the straight channel, with its center at $y = 0.15$. The molecules are tilted at $\approx 52°$ to the (010) mirror plane. It appears that up to $Q_{ads} = 4$ mol/uc, $C_2Cl_4$ molecules occupy only one kind of site of the silicalite-1 porosity. This unique

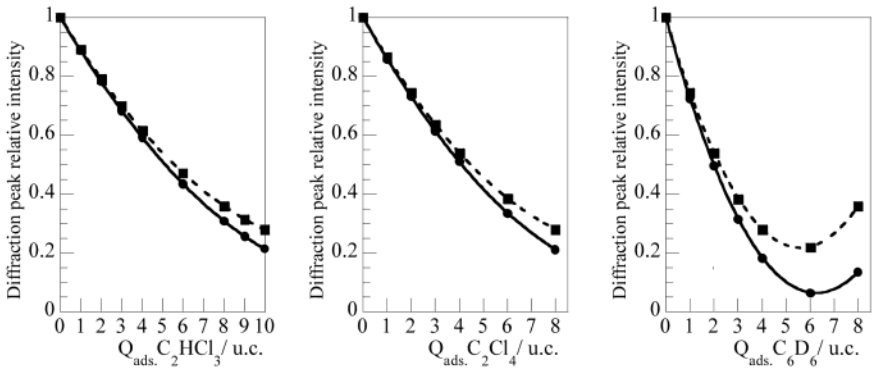


**Figure 9.** Relative intensity of the double diffraction peaks (101)(011) and (200)(020) as a function of $C_2HCl_3$, $C_2Cl_4$, and $C_6D_6$ loading, respectively, calculated for an homogeneous filling of the whole silicalite-1 porosity.

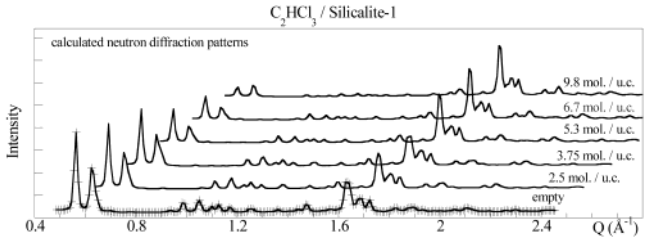


**Figure 10.** Calculated neutron diffraction patterns for increasing loading of $C_2HCl_3$ in silicalite-1 at 298 K.

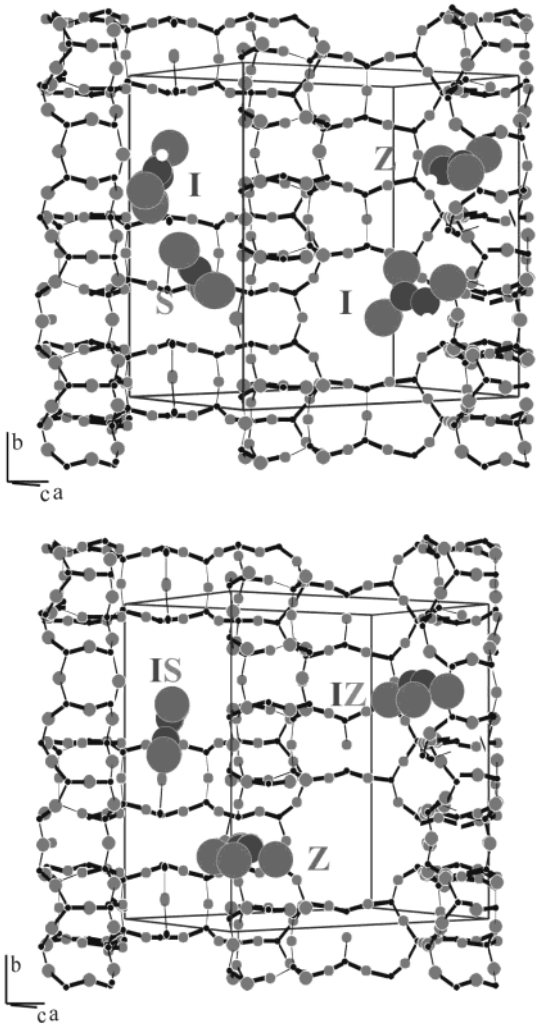


**Figure 11.** Possible locations of the three independent positions of $C_2HCl_3$ molecules within silicalite-1 porosity obtained from Rietvelt refinement of neutron diffraction patterns recorded at loading of $Q_{ads}$ = 1.2−3.75 mol/uc (top) and $Q_{ads}$ = 5.3−9.8 mol/uc (bottom).

position observed at low loading could be related to the strong coupling between the $C_2Cl_4$ molecule and the silicalite network.

At a higher loading, at $Q_{ads}$ = 5.0, 6.0, 7.2, and 8.0 mol/uc, respectively, $C_2Cl_4$ molecules occupy three independent locations with the same ratio of occupancy (Figure 14).

The first one is between the channel intersection and the straight channel at $y = 0.18$ and is parallel to the (010) mirror plane (IS). The second one in the straight channel at $y = 0.05$ is tilted at 66° to the (010) mirror plane (S). The third one in the zigzag channel is at $y = 0.21$ and lies parallel to the (010) mirror plane (Z). At $Q_{ads}$ = 8.0 mol/uc, the occupancies are 2.8, 2.3, and 2.9 per unit cell, respectively. It means that at higher loading, $C_2Cl_4$ molecules are reoriented and occupy the three kinds of sites as observed for $C_2HCl_3$ molecules.

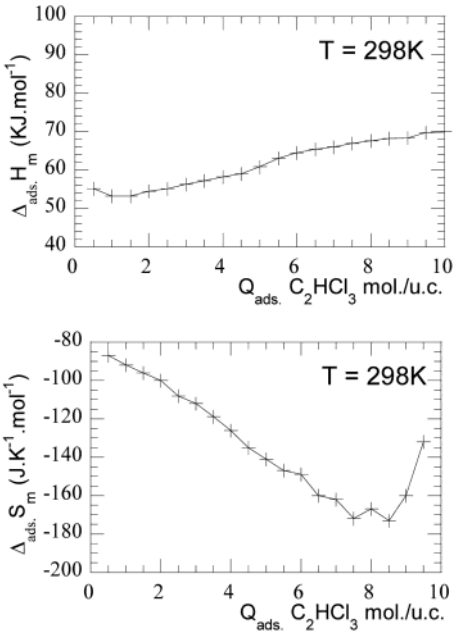


**Figure 12.** Relative absorption enthalpy for $C_2HCl_3$ in ZSM-5 reported by Bouvier et a1.[15,17]

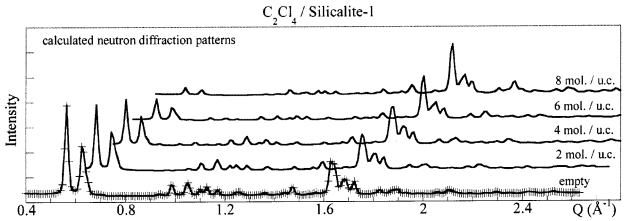


**Figure 13.** Calculated neutron diffraction patterns for increasing loading of $C_2Cl_4$ in silicalite-1 at 298 K.

These findings can be related to the calorimetric results obtained by Bouvier et al.[15,17] As shown in Figures 1 and 15, steps are observed at $Q_{ads}$ = 4 mol/uc in the isotherm, adsorption enthalpy, and adsorption entropy.

Up to $Q_{ads}$ = 4 mol/uc, the localization of the adsorbed molecules is near the channel intersections, giving rise to a continuous increase of enthalpy and continuous decrease of entropy. With such a stable configuration of the molecules, the adsorption phenomenon is blocked and it could go on only if the system gets enough chemical potential. From $Q_{ads}$ = 4−8 mol/uc, adsorbed molecules occupy the three kinds of sites in an organized arrangement corresponding to a large coupling between themselves and the silicalite. Their higher confinement (the loss of vibrational freedom) leads to a plateau of more negative entropy. It appears that in the case of $C_2Cl_4$, calorimetric features clearly correspond to a two step process of the silicalite porosity filling. This two step filling process is not related to silicalite phase transition MONO−ORTHO although occurring at the very same loading. The results obtained in the case of $C_2HCl_3$ adsorption support this assertion. Comparing the shape of these two chloroalkenes of similar size, the two step filling process takes place in the case of the symmetric $C_2Cl_4$ molecule, and then it can be seen as a consequence of the sensitivity between the symmetry of the sorbed molecule and the silicalite network.

The $C_2Cl_4$ positions found in this in situ neutron diffraction study are not in agreement with those recently determined by Mentzen et al.[29] in an ex situ X-ray diffraction study on H−ZSM-5. At $Q_{ads}$ = 4 mol/uc, $C_2Cl_4$ is at only one position centered in the channel intersection at $y = 0.26$ and oriented

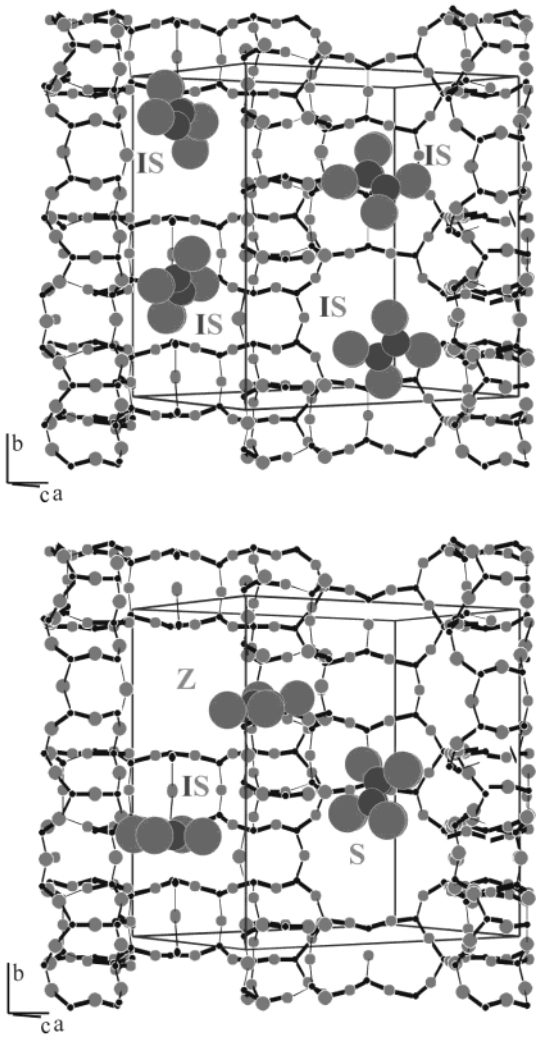


**Figure 14.** Possible locations of the three independent positions of $C_2Cl_4$ molecules within silicalite-1 porosity obtained from Rietvelt refinement of neutron diffraction patterns recorded at loading $Q_{ads}$ = 1.1−4.0 mol/uc (top) and $Q_{ads}$ = 5.0−8.0 mol/uc (bottom).

nearly perpendicular to the (010) mirror plane. At $Q_{ads}$ = 8 mol/uc, $C_2Cl_4$ is at its first position in the channel intersection and at a second position centered in the zigzag channel at $y = 0.25$ and oriented parallel to the (010) mirror plane. Neutron diffraction patterns calculated from these $C_2Cl_4$ positions reported by Mentzen[29] are compared with our neutron experimental patterns in Figure 16.

For each loading, a large intensity difference is observed for the two first highest peaks located at a very low angle. It comes out that the discrepancy in the adsorbed molecule locations is directly related to the experimental data and not due to different interpretations. This statement highlights that experimental adsorption results in silicalite depend largely on the origin of the sample used (its composition: completely siliceous or not, desaluminated or not, ..., its sorption capacity: amount of closed pores...) and on the type of the analysis performed (ex situ or in situ measurements).

**Case of $C_6D_6$.** Figures 3 and 17 show the experimental patterns for $C_6D_6$/silicalite system recorded at increasing loading and patterns resulting from Rietvelt refinement. At low loading, at $Q_{ads}$ = 1.0, 2.0, 3.0, and 4.0 mol/uc, respectively, $C_6D_6$ molecules converge to two independent locations. Up to $Q_{ads}$ = 2 mol/uc, both stand between channel intersection and straight channel with an equal occupancy. Their centers are at $y = 0.15$ and $y = 0.16$ and the molecules are tilted at ≈60° to the (010)

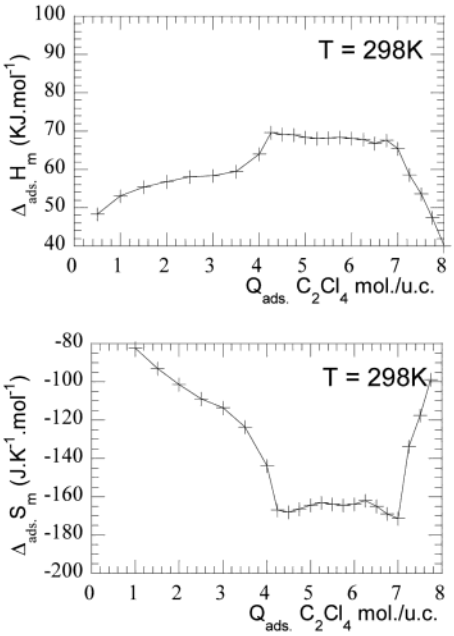


**Figure 15.** Relative absorption enthalpy and entropy for $C_2Cl_4$ in ZSM-5 reported by Bouvier et a1.[15,17]

mirror plane. From $Q_{ads}$ = 2−4 mol/uc, both locations are slightly moved to channel intersection center at $y = 0.22$ and $y = 0.23$ ($I_1$ and $I_2$ in Figure 18), with respective occupancy of 2.2 and 1.8. The molecule orientation is inclined at ≈70° and at ≈50° from the mirror plane, respectively. It appears that up to $Q_{ads}$ = 4 mol/uc, $C_6D_6$ molecules occupy channel intersections with two mutually exclusive locations. This particular arrangement of the molecules observed at low loading expresses the large coupling between the $C_6D_6$ molecule and the silicalite network.

At medium loading, at $Q_{ads}$ = 4.9 and 6.0 mol/uc, respectively, $C_6D_6$ molecules occupy four independent locations. At $Q_{ads}$ = 6.0 mol/uc, the occupancies are 2.0, 2.0, 1.0, and 1.0 per unit cell, respectively (Figure 18). Four molecules stand in the two previous locations ($I_1$, $I_2$) in the channel intersection (a very slight shift is observed). The two added molecules occupy two other locations with the same occupancy. The first one is between channel intersection and straight channel at $y = 0.12$ and the molecule is tilted at ≈75° to the mirror plane (IS). The second one is in the zigzag channel at $y = 0.24$ and the molecule lies nearly parallel to the (010) mirror plane (Z). Each of the two added molecules is very close from one in the channel intersection and is in a nearly orthogonal orientation. Such a set of two orthogonal molecules looks like a dimer. Then, from $Q_{ads}$ = 4−6 mol/uc, there is no change for $C_6D_6$ molecules located in the channel intersection. Added molecules occupy the two other kinds of site and form dimers like with the previous ones.

At a higher loading, at $Q_{ads}$ = 6.7, 7.5, and 8.0 mol/uc, respectively, $C_6D_6$ molecules occupy four independent locations (Figure 19). Four molecules are located between the channel intersection and the straight channel at $y = 0.13$ and at $y = 0.17$, respectively. Their orientation is either inclined at ≈75° or ≈ perpendicular to the (010) mirror plane ($IS_1$ and $IS_2$). The other molecules are either in the straight channel at $y = 0.01$ with an inclination of ≈50° (S) or in the zigzag channel at $y = 0.20$ with an inclination of ≈75° (Z). At $Q_{ads}$ = 8.0 mol/uc, the four locations have the same occupancy. From $Q_{ads}$ = 6−8 mol/uc, $C_6D_6$ molecules occupy the three kinds of sites, in a new homogeneous arrangement forming monomer chain links.

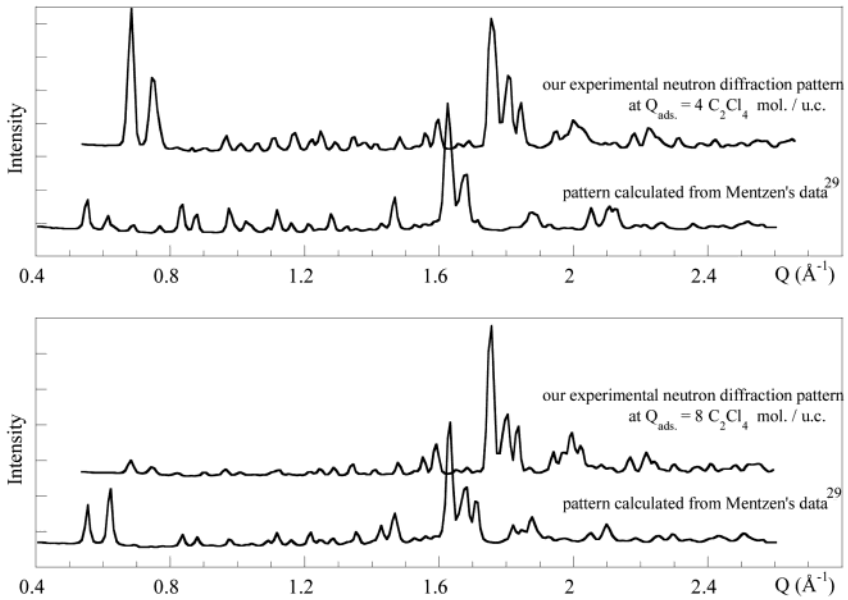


**Figure 16.** Our experimental neutron diffraction patterns of $C_2Cl_4$/silicalite-1 and patterns calculated from Mentzen's data[29] for the two loadings $Q_{ads}$ = 4 and 8 $C_2Cl_4$ mol/uc, respectively.

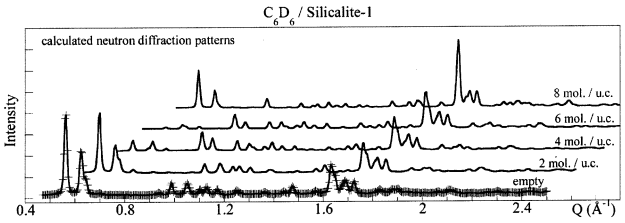


**Figure 17.** Calculated neutron diffraction patterns for increasing loading of $C_6D_6$ in silicalite-1 at 273 K.

The four previous molecules located in the intersections are displaced near the straight channels, and the two previous dimers are dissociated to be more in the center of the straight channels and the zigzag channels. These findings show that the two steps observed in the adsorption isotherms previously reported[12] (Figure 1) are the signatures of a three stage process of the porosity filling. Up to $Q_{ads}$ = 4 mol/uc, molecules fill the silicalite porosity up to be stabilized in the intersections. At $Q_{ads}$ = 6 mol/uc, the two added molecules take place in the straight and zigzag channels to form dimers with the previous molecules set in the intersections. At the higher loading of $Q_{ads}$ = 8 mol/uc, the molecules occupy the three types of sites in a new arrangement of interconnecting monomer chains.

As previously concluded in the case of $C_2HCl_3$ and $C_2Cl_4$, the steps in isotherms are not related to silicalite phase transitions MONO−ORTHO and ORTHO−PARA, these structural transitions arising as a consequence of the porosity filling whatever is the sorbed molecule. The location of $C_6H_6$ or $C_6D_6$ adsorbed into silicalite-1 or ZSM-5 has been widely investigated by many researchers using different experimental techniques. Up to the loading $Q_{ads}$ = 4 mol/uc, the $C_6D_6$ positions found in this in situ neutron diffraction study are in good agreement with structural results reported first by Mentzen et al.[30] and those recently determined by Goyal et al.[19] in a combined ex situ X-ray and neutron diffraction study on H−ZSM-5. For higher loading, $Q_{ads}$ > 4 mol/uc, our results are different from the results of Mentzen et al.[30] and from many experimental and theoretical others[9−13] where interpretations seem to more or less rely on these very first structural results published by Mentzen et al.[30] There are discrepancies for the loadings $Q_{ads}$ = 6 and 8 mol/uc. At $Q_{ads}$ = 6 mol/uc, four molecules lie in the center of the channel intersection at $y$ = 0.25, nearly parallel to the mirror plane and the two others are at only one position centered in

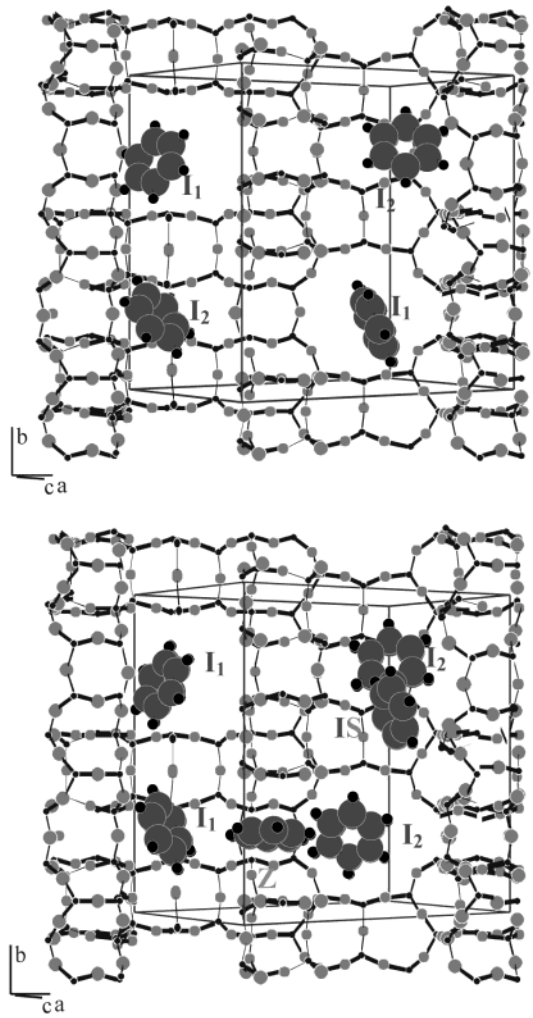


**Figure 18.** Possible locations of the independent positions of $C_6D_6$ molecules within silicate-1 porosity obtained from Rietvelt refinement of neutron diffraction patterns recorded at loading $Q_{ads}$ = 1.1−4.0 mol/uc (top) and $Q_{ads}$ = 4.9−6.0 mol/uc (bottom).

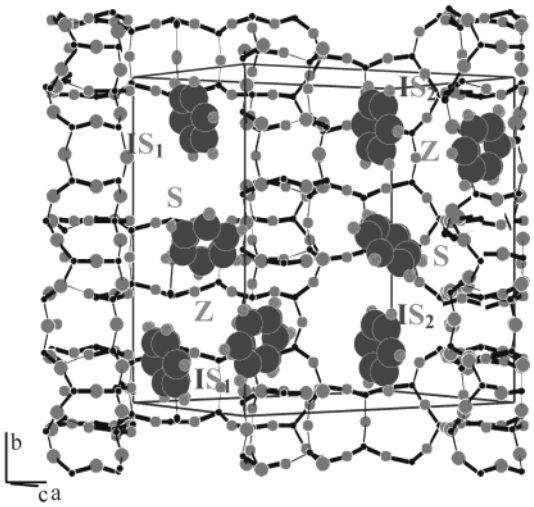


**Figure 19.** Possible locations of the four independent positions of $C_6D_6$ molecules within silicate-1 porosity obtained from Rietvelt refinement of neutron diffraction patterns recorded at loading $Q_{ads} = 6.7-8.0$ mol/uc.

the zigzag channel at $y = 0.25$ and oriented nearly perpendicular to the (010) mirror plane. At $Q_{ads} = 8$ mol/uc, $C_6H_6$ is at the first position in the channel intersection and at a second position centered in the straight channel at $y = 0$ and oriented perpendicular to the (010) mirror plane.

Neutron diffraction patterns calculated from the $C_6H_6$ positions reported by Mentzen[30] are compared with our neutron experimental patterns in Figure 20. For these loadings, a large intensity difference is observed either for the two first highest peaks or for the third highest peak. In addition, X-ray diffraction patterns reported in their last paper[30] exhibit a large diffraction bump at an angle that could be related to liquid $C_6H_6$. Consequently, the validity of the given loading $Q_{ads} = 6$ and 8 mol/uc could be questionable. As well, when comparing our results with those obtained by Goyal[19] for the loading $Q_{ads} = 7.6$ mol/uc (Figure 20), it appears that their $C_6D_6$ locations are more comparable with our positions found for the loading $Q_{ads} = 4.9-6$ mol/uc rather than those found for $Q_{ads} = 6.7-8$ mol/uc. Should these discrepancies be related to the origin (chemical composition) of the samples used that are either pure silicalite-1 or H−ZSM-5?

## 4. Conclusions

From our detailed in situ neutron diffraction study, we have investigated the structural properties of $C_2HCl_3$, $C_2Cl_4$, and $C_6D_6$ sorbed phases in silicalite-1. The obtained findings point out that steps observed in the type IV isotherm for large molecules are not signatures of phase transitions but are related to stages in the filling process induced by the three kinds of site of the silicalite porosity. In the case of $C_6D_6$, the filling mode is a three stage process (the $C_6D_6$ molecules fill successively, the intersections, the straight channels, and the sinusoidal channels by forming dimers and then interconnecting monomer chains). Concerning $C_2Cl_4$, it is a two stage process (the $C_2Cl_4$ molecules fill the intersections and after indifferently the straight channels and the sinusoidal channels). Usual sorption is observed for $C_2HCl_3$, which fills all parts of the silicalite-1 porosity indifferently. By analyzing our results and those reported in the literature, the stage-filling process seems to be molecule symmetry-dependent. It is promoted for high-symmetry molecules such as $C_2Cl_4$, $C_6H_6$ or $C_6D_6$, *p*-xylene. Vertical steps are observed in their isotherm, and they correspond to one or two stages of the filling process. It is reduced for low symmetry molecules such as toluene and ethylbenzene, and the steps observed in their isotherm are oblique and not so marked. It is inhibited for no symmetry molecules such as $C_2HCl_3$, there is no step in their isotherm, and the porosity-filling process is more homogeneous on the three kinds of sites.

The discrepancies observed between our results and those obtained by many researchers on these systems point out that observations of the stage-filling process are very experiment-dependent. The origin of the sample used (its composition, quality, etc.), the type of the analysis performed, and if they are ex situ or in situ measurements appear to be highly sensitive factors for the adsorption process of tight-fitting molecules in silicalite-1, where the complex porosity is largely flexible and

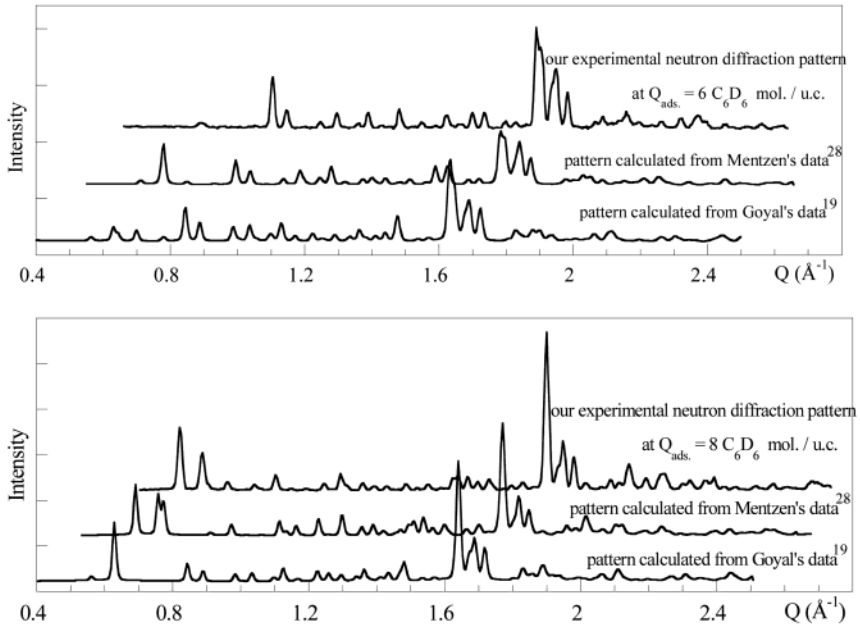


**Figure 20.** Our experimental neutron diffraction patterns of $C_6D_6$/silicalite-1 and patterns calculated from Sacerdote−Peronnet's data[28] ($C_6D_6$ positions given for $Q_{ads} = 6$ and 8 mol/uc) and Goyal's data[19] ($C_6D_6$ positions given for $Q_{ads} = 7.6$ mol/uc) for the two loadings $Q_{ads} = 6$ and 8 mol/uc, respectively.

silicalite structure-dependent. Our hope is that these experimental results added to those obtained very recently[10,19,24] will help to enhance simulation studies for a better understanding of adsorption phenomena in MFI zeolites.

## References and Notes

(1) Olson, D. H.; Kokotailo, G. T.; Lawton, S. L. *J. Phys. Chem.* **1985**, *85*, 2238.
(2) Talu, O.; Guo, C. J.; Hayhurst, D. *J. Phys. Chem.* **1989**, *93*, 7294.
(3) Thamm, H. *Zeolite* **1987**, *7*, 341.
(4) Müller, U.; Reichert, H.; Robens, E.; Unger, K.; Grillet, Y.; Rouquerol, F.; Rouquerol, J.; Dongfent P.; Mersmann, A. *Fresenius Z. Anal. Chem.* **1989**, *333*, 433.
(5) Llewellyn, P. L.; Coulomb, J. P.; Grillet, Y.; Patarin, J.; Lauter, H.; Reichert, H.; Rouquerol, J. *Langmuir* **1993**, *9*, 1846.
(6) Llewellyn, P. L.; Coulomb, J. P.; Grillet, Y.; Patarin, J.; André, G.; Rouquerol, J. *Langmuir* **1993**, *9*, 1852.
(7) Coulomb, J. P.; Martin, C.; Llewellyn, P. L.; Grillet, Y. *Stud. Surf. Sci. Catal.* **1997**, *105*, 2355.
(8) Coulomb, J. P.; Llewellyn, P. L.; Grillet, Y.; Rouquerol, J. *Stud. Surf. Sci. Catal.* **1994**, *87*, 535.
(9) Snurr, R. Q.; Bell, A. T.; Theodorou, D. N. *J. Phys. Chem.* **1993**, *97*, 13742.
(10) Huang, Y.; Havenga, E. A. *J. Phys. Chem. B* **2000**, *104*, 5084 and references therein.
(11) Clark, L. A.; Snurr, R. Q. *Chem. Phys. Lett.* **1999**, *308*, 155.
(12) Rudzinski, W.; Narkiewicz-Michalek, J.; Szabelshi, P.; Chiang, A. S. T. *Langmuir* **1997**, *13*, 1095.
(13) Du, Z.; Dunne, L. J.; Manos, G.; Chaplin, M. F. *Chem. Phys. Lett.* **2000**, *318*, 319.
(14) Song, L.; Sun, Z. L.; Rees L. V. C. *Stud. Surf. Sci. Catal.* **2001**, *1*, 153.
(15) Bouvier, F. Thesis, Université de Bourgogne, 1998.
(16) Lee, C.-K.; Chiang, A. S. T. *J. Chem. Soc., Faraday Trans.* **1996**, *92*, 3445.
(17) Bouvier, F.; Weber, G. *J. Therm. Anal.* **1998**, *54*, 881.
(18) Pope, C. G. *J. Phys. Chem.* **1986**, *90* (5), 835.
(19) Goyal, R.; Fitch, A. N.; Jobic, H. *J. Phys. Chem. B* **2000**, *104*, 2878.
(20) Van Koningsveld, H.; Van Bekkum, H.; Jansen, J. C. *Acta Crystallogr.* **1987**, *B43*, 127.
(21) Van Koningsveld, H.; Jansen, J. C.; Van Bekkum, H. *Zeolites* **1990**, *10*, 235.
(22) Van Koningsveld, H.; Tuinstra, F.; Van Bekkum, H.; Jansen, J. C. *Acta Crystallogr.* **1989**, *B45*, 423.
(23) Narkiewicz-Michalek, J.; Szabelshi, P.; Rudzinski, W.; Chiang, A. S. T. *Langmuir* **1999**, *15*, 6091.
(24) Song, L.; Rees, L. V. C. *Micropor. Mesopor. Mater.* **2000**, *35*−*36*, 301
(25) Rietveld, H. M. *J. Appl. Crystallogr.* **1969**, *2*, 65.
(26) François, V. Thesis, Université de Bourgogne, 2001.
(27) Mentzen, B. F.; Gelin, P. *Mater. Res. Bull.* **1995**, *30* (3), 373.
(28) Sacerdote-Peronnet, M.; Mentzen, B. F. *Mater. Res. Bull.* **1993**, *28*, 767.
(29) Mentzen, B. F.; Lefebvre, F. *C. R. Acad. Sci. Paris, Ser. IIc: Chim.* **2000**, *3*, 843.
(30) Mentzen, B. F.; Lefebvre, F. *Mater. Res. Bull.* **1997**, *22*, 813.